ACS Photonics
pubs.acs.org/journal/apchd5 Article

Improvement of the Emission Intensity of GaN-Based Micro-Light Emitting Diodes by a Suspended Structure

Yang Mei, Minchao Xie, Tao Yang, Xin Hou, Wei Ou, Hao Long, Leiying Ying, Yuejun Liu, Guoen Weng,* Shaoqiang Chen, and Baoping Zhang*

Cite This: *ACS Photonics* 2022, 9, 3967−3973 Read Online

ABSTRACT: Herein, suspended GaN-based micro-light emitting diodes (LEDs) are ingeniously proposed and fabricated, showing a substantially enhanced light emission compared to conventional micro-LEDs on the sapphire substrate. The suspended architecture is prepared by transferring epitaxial layers to micrometal pillars on the copper plate after removing the original sapphire substrate. The photoluminescence intensity of the suspended micro-LED exhibits 150% higher than that of the normal device, and the electroluminescence intensity is increased by 114% in the current injection range of 0−10 mA. The enhancement of the output intensity benefits from the partially relaxed strain of the epitaxial film and the resultant reduction of the quantum confined Stark effect in the InGaN quantum well active region, as well as the improved light extraction efficiency due to the larger light-escaping area and less optical absorption and trapping, which are unambiguously verified by Raman spectroscopy and ray-tracing simulations. This study provides a new promising route to design and fabricate highly efficient micro-LEDs for practical applications.

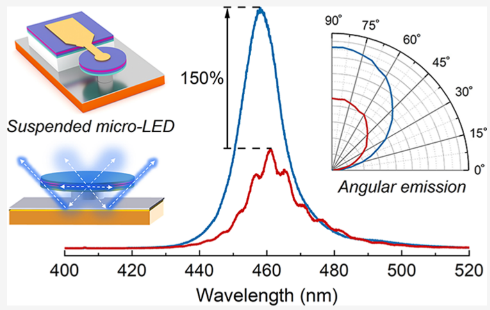

KEYWORDS: *GaN-based micro-LED, suspended device mesa, large light extraction efficiency, strain relaxation*

1. INTRODUCTION

GaN-based micro-light emitting diodes (LEDs) take the advantages of high resolution, low power consumption, high refresh rate, and high brightness, so they have great commercial potential for applications in displays.[1−4] GaN-based micro-LEDs are also featured with a much larger bandwidth and faster frequency response than the typical LED, which make them an ideal light source for visible light communication (VLC). In the LED applications, the overall external quantum efficiency (EQE) plays a crucial role, which is dominantly determined by the internal quantum efficiency (IQE) and the light extraction efficiency (LEE). However, the IQE of GaN-based micro-LED is limited by the quantum confined Stark effect (QCSE) in the InGaN/GaN quantum wells (QWs) originating from the internal piezoelectric and spontaneous polarizations.[5,6] On the other hand, the LEE of GaN-based LEDs is usually low because most of the light emitted from the active region remains trapped in the LED mesa and substrate because of the total internal reflection at the GaN/air and sapphire/air interfaces.[7] Light trapping further enhances photon reabsorption in the active region, resulting in the reduction of the output intensity. In order to reduce the QCSE in the InGaN QWs, one straightforward approach is growing the InGaN/GaN QWs on nonpolar or semipolar substrates.[8−12] However, such freestanding GaN substrates are usually expensive, making them unsuitable for mass production. Moreover, it is known that the strain depends on the size of LED chips. By shrinking the size of the device to the nano-range, the strain can be partially relaxed and the QCSE can be reduced to some degree.[13,14] However, this method will inevitably increase the specific surface area of the device, and the defect on the sidewall will induce nonradiative recombination, limiting the IQE of the device. Although micro-LEDs present an improved LEE compared to those large-area LEDs due to their smaller size of device mesa, which will reduce the lateral propagation of the light and increase the ratio of escaping surface area to light generation area, a large amount of light is still trapped in the thick sapphire substrate for the conventional micro-LED structure. For the micro-LEDs on Si, they even suffer additional serious light absorption by the substrate, resulting in the further limitation of their LEE.[15−17] At present, the most common methods to improve the LEE of GaN-based micro-LEDs reform the sidewall and light reflection surfaces, including dielectric sidewall passivation,[18] surface and sidewall roughening or inclining,[19,20] using patterned sapphire substrates,[21,22] fabrication of nanoscale period structures on the surface,[23,24] and so forth. These

Received: September 1, 2022
Published: November 29, 2022

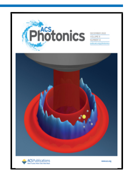

https://doi.org/10.1021/acsphotonics.2c01366
ACS Photonics 2022, 9, 3967−3973

methods, however, cannot effectively extract the light that propagates toward the bottom substrate and usually can only make 10−20% improvements in LEE. In 2020, Liu et al. fabricated a semi-floating GaN-based LED array with mesa of the device separated from the Si substrate. Light absorption by the Si substrate can be eliminated, and the photoluminescence (PL) intensity showed a 150% improvement.[25] However, the device can only operate under optically pumped conditions and no electrical injection was realized. Therefore, a more effective method needs to be developed to enhance the LEE and output intensity of GaN-based micro-LEDs.

In this study, GaN-based micro-LEDs with a suspended architecture were fabricated. Such a suspended structure is usually used in the optically pumped whispering gallery mode (WGM) lasers,[26] but the electrically injected light-emitting devices and the influence of suspended structures on the performance of GaN-based micro-LEDs have barely been reported. Here, we demonstrated both experimentally and theoretically that the suspended structure can significantly reduce the QCSE in the InGaN QWs and boost the LEE simultaneously. The sapphire substrate used for material growth was removed by laser lift off (LLO), and the epitaxial layers were transferred to a copper plate with Cr mirror and supported by micro-metal pillars. The peripheral area of the mesa of the micro-LED was suspended from the substrate, forming the so-called suspended micro-LED. The residual strain in the GaN layer is partially relaxed, leading to a smaller QCSE in the InGaN multiple QWs (MQWs) compared to the normal micro-LEDs with the sapphire substrate. The LEE is enhanced because of the enlarged light-escaping surface. Apart from the top surface and side wall, light can also escape from the suspended mesa through the bottom surface and then be reflected by the Cr mirror. The PL intensity of the suspended micro-LED is 2.5 times that of the normal micro-LED (increased by 150%), and the electroluminescence (EL) intensity is increased by 114% in the injection current range of 0−10 mA. Raman spectroscopy and band diagram calculation were conducted to reveal the effect of strain relaxation on the InGaN QW active region, and the ray-tracing simulations further verified the enhancement of LEE in the suspended micro-LED. This study provides a new promising method to design and fabricate highly efficient micro-LEDs for future applications.

2. MATERIALS AND METHODS

The epitaxial wafer used in this study was grown on a (0001)-oriented sapphire substrate by metal−organic chemical vapor deposition (MOCVD), and the active region contains three pairs of $In_{0.18}Ga_{0.82}N$/GaN (2.5/6 nm) MQWs (detailed information about the epitaxial wafer is given in the Supplementary Material, part 1). The device fabrication process is illustrated in Figure 1a. A 30-nm-thick indium tin oxide film (ITO) was first deposited on the epitaxial wafer as the current spreading and ohmic-contacting layer (Step 1). A 1.5-μm-thick SiO_2 layer was then deposited and holes with a diameter of 10 μm were opened to expose the ITO layer (Step 2). In step 3, Cr/Au (40/180 nm) layers were deposited and a 200-μm-thick copper plate was electroplated on the surface. The Cr/Au layers and the copper plate filled the holes in the SiO_2 layer, contacting directly with the ITO. The micro-metal pillars inside the SiO_2 holes will support the suspended LED and act as the current injection path after the whole fabrication process. The sapphire substrate was subsequently removed by LLO, and the epitaxial film was thinned to ~1 μm by chemical−mechanical polishing (CMP) without damaging the crystal quality of the active region (Step 4).[27,28] The mesa of the micro-LED with a diameter of 25 μm was formed by inductively coupled plasma (ICP) etching, and the etching process stopped when the SiO_2 layer under the GaN film was exposed (Step 5). It should be noted that a squared mesa near the LED was also formed during this step to locate the contacting pad. At last, the sacrificial SiO_2 layer under the LED mesa was removed by hydrofluoric acid solution (HF) wet etching, forming the suspended structure (Step 6). SiO_2 under the contacting pad will also be undercut for a little during this step, but most of the SiO_2 can be retained by controlling the etching time because the mesa of the micro-LED is smaller than the contacting pad. An air-bridge-type Cr/Au electrode was finally fabricated for the convenience of device characterization. Current can be injected into the device vertically through the top electrode and the copper substrate, avoiding the current crowding effect in normal LEDs with a lateral injection scheme.[29] The copper substrate can also improve the thermal dissipation of the suspended device.[30,31] Figure 1b−d shows the scanning electron microscopy (SEM) images of the fabricated suspended device, from which the air-bridge electrode and the air gap underneath the mesa of the micro-LED can be observed. The height of the supporting copper pedestal is too small (1.5 μm) compared to the size of the mesa of the device (25 μm), so it cannot be seen from the SEM image. It should be noted that the suspended mesa of the device can be easily cracked or broken by the electrical probe, and the air-bridge electrode and n-contacting pad here are mainly for the convenience of the probe measurement during electrical injection, similar to J. Wang's work.[32] The relatively large n-contacting pad seems to limit the density of the micro-LED array. However, for future real device applications, such a large n-contacting pad is not necessary, and a smaller

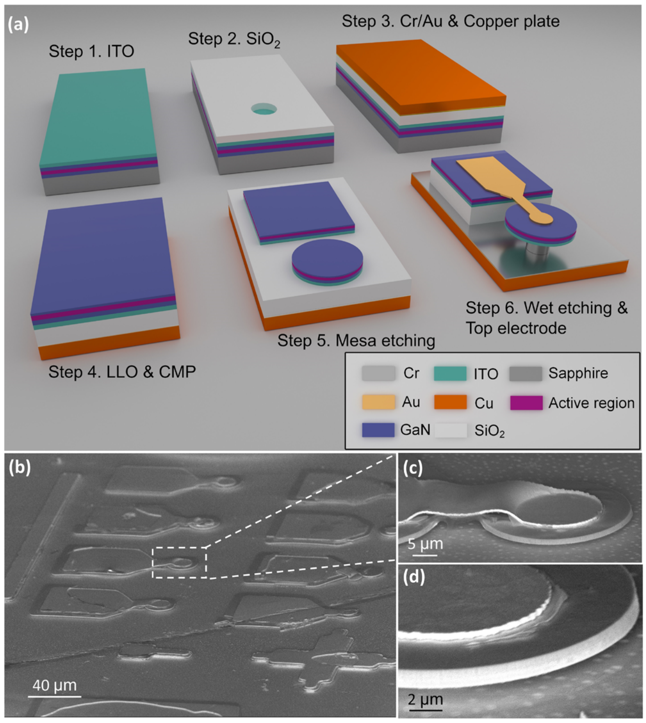

Figure 1. (a) Fabrication process of the suspended micro-LED. (b−d) SEM images of the fabricated devices.

https://doi.org/10.1021/acsphotonics.2c01366
ACS Photonics 2022, 9, 3967−3973

contacting pad and wire connection can be used to ensure high resolution.

3. RESULTS AND DISCUSSION

To study the optical characteristics of the suspended micro-LED, PL measurement was first conducted using a micro-PL system before the top electrode was deposited. The mesa of the micro-LED was excited by a continuous wave 405 nm laser diode focused by an objective lens (10×, NA0.35). The output of the micro-LED was collected by the same objective lens and guided to the spectrometer through a free space optical path. For comparison, PL spectra of the original epi-wafer and a normal micro-LED fabricated on sapphire without the suspended structure were also measured, as shown in Figure 2a. The intensity of the normal micro-LED is slightly higher

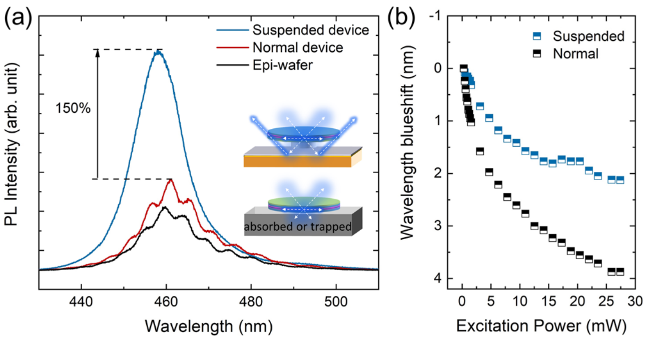

Figure 2. (a) PL spectra of the epi-wafer, normal micro-LED, and suspended micro-LED. Inset shows the light extraction mechanism in different structures. (b) Power-dependent peak movement of the normal and suspended micro-LEDs.

than that of the original epi-wafer, which is mainly due to the light escaping from the sidewall. Surprisingly, the intensity of suspended micro-LED increases dramatically and is nearly 2.5 times (increase by 150%) that of the normal micro-LED. The suspended structure can effectively increase the LEE of GaN-based micro-LED by a much larger light-escaping area. Light emitted by the active region can also be extracted from the bottom surface of the GaN membrane and then be reflected by the Cr mirror on the copper substrate (reflectivity of a 40 nm thick Cr layer is ~70% at 457 nm, see Supplementary Material, part 2). Metal layers with much higher reflectivity, such as silver and aluminum, can be used in further work. In addition, light trapping by the sapphire substrate can also be eliminated in the suspended structure. The schematic mechanism of enhanced light extraction in suspended micro-LED is illustrated in the inset of Figure 2a. Moreover, it is shown that the spectral full width at half maximum (FWHM) of the suspended device is ~18 nm, smaller than that of the normal device (21 nm), and the emission peak (457.8 nm) exhibits a slight blueshift compared to those of the epitaxial wafer and the normal micro-LED (461.4 nm). Such spectral blueshift and smaller FWHM can be attributed to the strain relaxation caused by the removal of the sapphire substrate. As is well known, GaN grown on a lattice-mismatched sapphire substrate suffers compressive strain, which will induce more serious QCSE in the following grown InGaN QW active region.[33] When the sapphire is lifted off, the residual compressive stress is reduced; thus, the QCSE and the band tilt of the InGaN QW can be weakened, leading to the spectral blueshift and narrowing. Figure 2b presents the excitation power-dependent spectral peak positions for both devices. Clear blueshift caused by the screening of QCSE and band filling can be observed. The peak movement for the suspended structure is much smaller, reflecting the smaller strain in the GaN film after LLO. The exciton recombination characteristics of the two structures were studied by the low temperature (77 K) time-resolved PL (TRPL) measurement under impulsive picosecond (ps) optical pumping at 405 nm, as shown in Figure 3. The decay

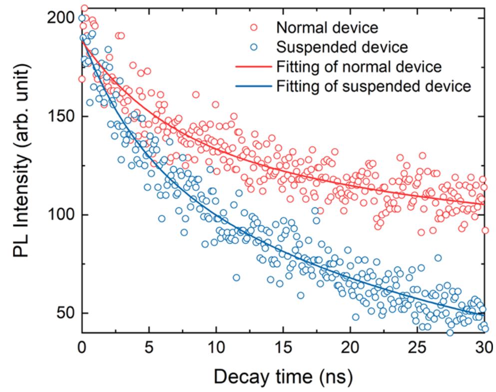

Figure 3. TRPL decay curve of the normal and suspended micro-LEDs at 77 K.

curves were fitted with a double exponential model that can be described as follows:[34]

$$I(t) = A + \alpha_1 \exp\left(-\frac{t}{\tau_1}\right) + \alpha_2 \exp\left(-\frac{t}{\tau_2}\right) \quad (1)$$

where A is a constant, α_1 and τ_1 (or α_2 and τ_2) are defined as the fast (or slow) decay component.[34] τ_1 and τ_2 extracted from fitting results are 4.1 and 25.7 ns for the suspended device and 6.1 and 36.2 ns for the normal device, respectively. The fast carrier decay for the suspended sample indicates the weaker QCSE and the resultant larger overlap of electron and hole wave functions after the strain relaxation.

The release of the compressive stress for the suspended LED was experimentally verified by Raman spectroscopy, as shown in Figure 4a. The Raman E_{2h} mode for the suspended device and the epi-wafer locates at 570.58 and 567.97 cm^{-1}, respectively, showing a 2.61 cm^{-1} decrease. This means an increase in the in-plane lattice constant of GaN after removing

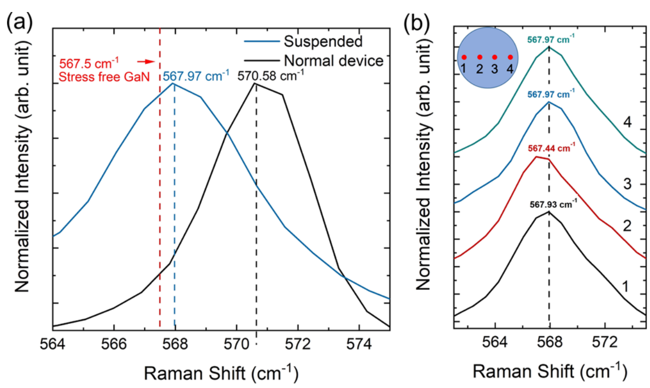

Figure 4. (a) Raman spectra of the suspended device and original epi-wafer. (b) Raman spectra from four different points of the suspended device.

https://doi.org/10.1021/acsphotonics.2c01366
ACS Photonics 2022, 9, 3967−3973

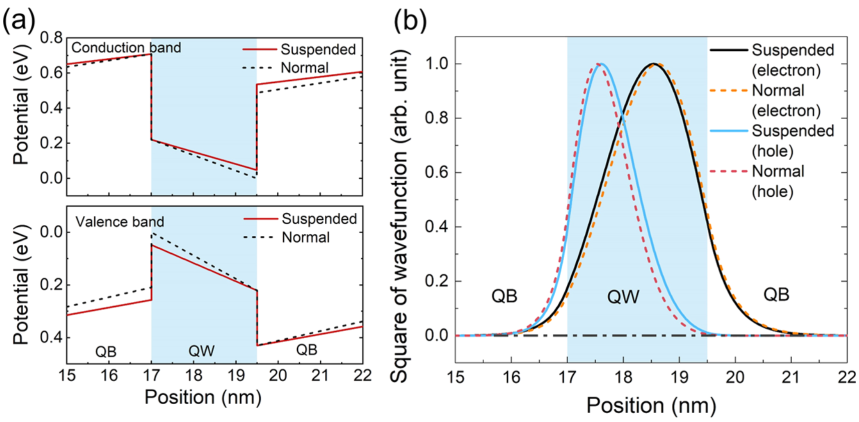

Figure 5. (a) Calculated band diagram of the suspended and normal devices. (b) Normalized electron and hole wave functions of the suspended and normal devices.

the sapphire substrate. The residual in-plane compressive stress can be calculated by $\Delta\omega = a_{GaN}\sigma_{XX}$, where $\Delta\omega$ is the shift of the phonon frequency with respect to that of stress-free GaN (567.5 cm^{-1}), a_{GaN} is the Raman stress coefficient of GaN (2.56 cm^{-1} GPa^{-1}), and σ_{XX} is the in-plane compressive stress.[25] Accordingly, the residual compressive stress in the original epi-wafer and the suspended device turn out to be 1.24 and 0.19 GPa, respectively. The uniformity of the strain distribution in the suspended mesa was explored by measuring the Raman frequency at four different points (denoted as 1, 2, 3 and 4), as shown in Figure 4b. The different points (see the inset) present similar Raman peak positions, indicating satisfactory homogeneity in residual in-plane compressive strain.

The strain is partially relaxed in the GaN of the suspended device, which will also influence the strain state and then the QCSE of the InGaN QWs grown on it. Since the QW layer is very thin and the indium content is not high, the InGaN QW can be assumed to be grown coherently on the GaN template, and the a-axis lattice constant of both InGaN well layers and GaN are identical.[35] With the experimentally obtained strain state in the GaN layer, we can calculate the a-axis length of GaN and then study the strain and polarization-induced band bending in InGaN QWs. For theoretically clarifying the strain relaxed effect, a self-consistent Poisson-Schrodinger coupling model was used to calculate the energy band structure of the InGaN/GaN quantum wells (see Supplementary Material, part 3). As shown in Figure 5a, the band structure of QW is less inclined in the suspended device. This is because the sapphire substrate is removed and the compressive strain is relaxed in the GaN layer. The larger a-axis length of the GaN layer reduces the lattice mismatch between InGaN QW and GaN, resulting in a weaker QCSE. Meanwhile, such tilt-attenuated energy band structure gives rise to a blueshift of the emission wavelength, as seen in Figure 2a. More importantly, the smaller QCSE can increase the overlap between the electron and hole wave functions by ~20% (Figure 5b), which results in a larger exciton transition probability and a higher carrier recombination rate (see Figure 3) and finally contributes to the improvement of IQE[36] and exciton oscillator strength in the suspended structure.

The EL characteristics of the suspended device were studied after the fabrication of the top air-bridge type electrode. Figure 6a shows the typical current versus voltage (IV) curve and emission profile of the suspended device. The bias voltage

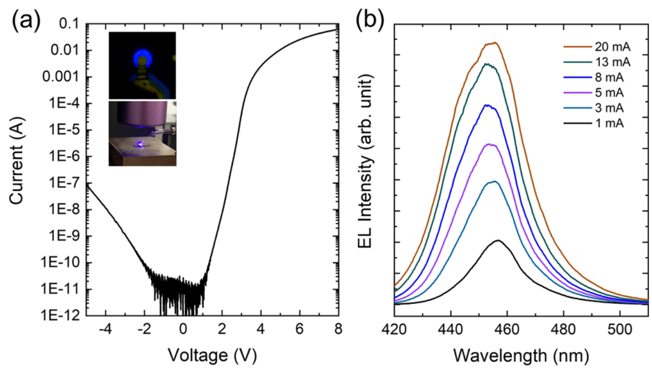

Figure 6. (a) IV curve and emission profile of the suspended device. (b) EL spectra of the suspended device under different currents.

under 20 mA is 5.7 V, and the reverse leakage current under a bias voltage of −5 V is ~90 nA, which are among the typical values for GaN-based micro-LEDs.[37,38] Figure 6b shows the current-dependent EL spectra of the suspended device. With the injection current increasing from 1 to 20 mA, the central wavelength of the EL spectra shows a slight blueshift from 456.7 to 452 nm, and the FWHM increases from 20 nm to 32 nm because of the band-filling effect. Figure 7 exhibits the output power and relative EQE as a function of current for the suspended and normal micro-LEDs, respectively. The output power of the suspended device is 1.85 mW under 10 mA

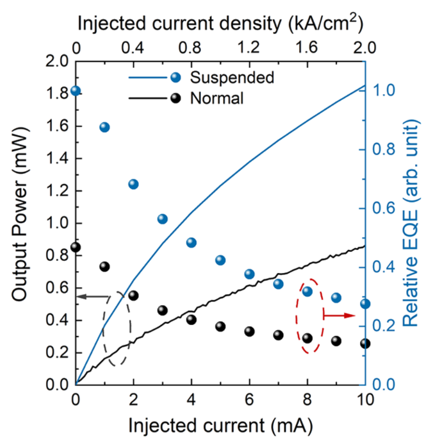

Figure 7. Output power and relative EQE as a function of the current.

https://doi.org/10.1021/acsphotonics.2c01366
ACS Photonics 2022, 9, 3967−3973

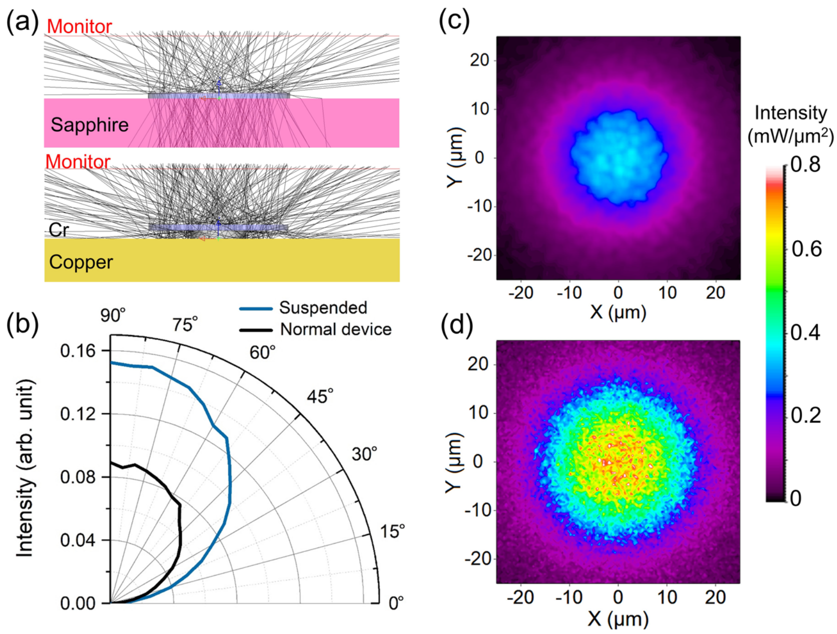

Figure 8. (a) Ray-tracing profile of the normal and suspended devices. (b) Angular-dependent emission intensity of the normal and suspended devices. (c,d) Intensity distribution patterns of the normal and suspended devices.

(corresponding to a current density of 2 kA/cm^2), more than 2 times that of the normal micro-LED (0.86 mW). Similarly, the EQE of the suspended device is much larger than that of the normal micro-LED in this current range, which is mainly attributed to the smaller QCSE and the larger LEE. We note that the EQE of the suspended device decreases a bit more rapidly with increasing current density, and this may be caused by the higher thermal effect in the suspended device. Although the copper substrate can help extract heat energy out of the device, the air gap between the GaN membrane and the substrate shrinks the effective thermal dissipation area.[39] Thermal dissipation of the suspended device can be improved by increasing the diameter of the supporting micropillar in further work (see Supplementary Material, part 4).

To assess how LEE is improved by the device structure, Monte Carlo ray-tracing simulations were conducted. The radiation emission in the active QWs was modeled as a 10-nm-thick volumetric source where 10^6 monochromatic rays (λ = 458 nm) were generated with a uniform distribution of emission directions, and the input power was fixed at 1 W. The top electrode was not considered in the model, and the sapphire/air interface at the backside of the normal device was modeled as a rough surface (an ideal Lambertian scattering profile) because the sapphire substrate used for material growth is single-plane polished. Detailed parameters for the materials used in the simulation can be found in the Supplementary Material, part 5. Figure 8a shows the simulated ray-tracing profile of the normal and suspended devices, and the LEE is proportional to the number of rays out of the surface. It can be clearly observed that more rays can be extracted from the suspended device and detected by the monitor above the device, benefiting from the extraction of the bottom mesa surface, the reflection of the metal mirror, and the absence of substrate trapping. The calculated angular-dependent emission intensities from the front side into the air are shown in Figure 8b. The emission patterns show Lambertian distribution for both devices, and the output intensity increases for all angles as the suspended structure is used. The divergence angle shows no identifiable difference between the two structures (see Supplementary Material, part 5). The front-side LEEs were derived to be 47.7 and 28.3% for the suspended and normal devices, respectively, and the diameter of the device mesa does not show much influence on the LEE of the suspended device (see Supplementary Material, part 5). Figure 8c,d shows the calculated emission pattern collected by the monitor above the surface of the device. It is clearly revealed that the luminous flux of the suspended device is much more remarkable than that of the normal device. Conclusively, the simulations confirm that LEE can indeed be improved by the suspended device structure.

4. CONCLUSIONS

In summary, we have fabricated GaN-based micro-LEDs with a novel suspended architecture, in which the IQE and LEE can be effectively improved. Compared to those micro-LEDs with the normal structure, the output power of the suspended devices can be increased by 114% in the injection current range of 0−10 mA. The mechanisms of the performance improvement are the enlarged light-escaping area of the suspended structure and the attenuated QCSE of the active region caused by the removal of the sapphire substrate. Raman spectroscopy and ray-tracing simulations were also conducted to further verify the reduced strain and enhanced LEE in the suspended micro-LED. This study provides an effective method to improve the performance of GaN-based micro-LEDs.

■ ASSOCIATED CONTENT

Supporting Information

The Supporting Information is available free of charge at https://pubs.acs.org/doi/10.1021/acsphotonics.2c01366.

Detailed information of the epitaxial wafer, simulated reflective spectrum of the Cr mirror, Poisson−Schrodinger coupling model used in this study, and

https://doi.org/10.1021/acsphotonics.2c01366
ACS Photonics 2022, 9, 3967−3973

detailed information about thermal dissipation and Monte Carlo ray-tracing simulation (PDF)

AUTHOR INFORMATION

Corresponding Authors

Guoen Weng − *State Key Laboratory of Precision Spectroscopy, Department of Electronic Engineering, East China Normal University, Shanghai 200241, China;* orcid.org/0000-0001-7786-2133; Email: egweng@ee.ecnu.edu.cn

Baoping Zhang − *Laboratory of Micro/Nano-Optoelectronics, Department of Micro Electronic and Integrated Circuits, Xiamen University, Xiamen 361005, China;* Email: bzhang@xmu.edu.cn

Authors

Yang Mei − *Laboratory of Micro/Nano-Optoelectronics, Department of Micro Electronic and Integrated Circuits, Xiamen University, Xiamen 361005, China;* orcid.org/0000-0001-7190-0338

Minchao Xie − *Laboratory of Micro/Nano-Optoelectronics, Department of Micro Electronic and Integrated Circuits, Xiamen University, Xiamen 361005, China*

Tao Yang − *Laboratory of Micro/Nano-Optoelectronics, Department of Micro Electronic and Integrated Circuits, Xiamen University, Xiamen 361005, China*

Xin Hou − *Laboratory of Micro/Nano-Optoelectronics, Department of Micro Electronic and Integrated Circuits, Xiamen University, Xiamen 361005, China*

Wei Ou − *Laboratory of Micro/Nano-Optoelectronics, Department of Micro Electronic and Integrated Circuits, Xiamen University, Xiamen 361005, China*

Hao Long − *Laboratory of Micro/Nano-Optoelectronics, Department of Micro Electronic and Integrated Circuits, Xiamen University, Xiamen 361005, China;* orcid.org/0000-0002-7057-7214

Leiying Ying − *Laboratory of Micro/Nano-Optoelectronics, Department of Micro Electronic and Integrated Circuits, Xiamen University, Xiamen 361005, China*

Yuejun Liu − *State Key Laboratory of Precision Spectroscopy, Department of Electronic Engineering, East China Normal University, Shanghai 200241, China*

Shaoqiang Chen − *State Key Laboratory of Precision Spectroscopy, Department of Electronic Engineering, East China Normal University, Shanghai 200241, China;* orcid.org/0000-0002-0458-3894

Complete contact information is available at:
https://pubs.acs.org/10.1021/acsphotonics.2c01366

Funding

This work was supported by the National Key Research and Development Program of China (No. 2017YFE0131500), the National Natural Science Foundation of China (Nos. 62104204, U21A20493), and the President's Foundation of Xiamen University (No. ZK1044).

Notes

The authors declare no competing financial interest.

REFERENCES

(1) Anwar, A. R.; Sajjad, M. T.; Johar, M. A.; Hernández-Gutiérrez, C. A.; Usman, M.; Łepkowski, S. Recent Progress in Micro-LED-Based Display Technologies. *Laser Photonics Rev.* **2022**, *16*, No. 2100427.

(2) Huang, Y.; Hsiang, E. L.; Deng, M. Y.; Wu, S. T. Mini-LED, Micro-LED and OLED displays: Present status and future perspectives. *Light: Sci. Appl.* **2020**, *9*, 105.

(3) James Singh, K.; Huang, Y. M.; Ahmed, T.; Liu, A. C.; Huang Chen, S. W.; Liou, F. J.; Wu, T.; Lin, C. C.; Chow, C. W.; Lin, G. R.; Kuo, H. C. Micro-LED as a promising candidate for high-speed visible light communication. *Appl. Sci.* **2020**, *10*, 7384.

(4) Wu, T.; Sher, C. W.; Lin, Y.; Lee, C. F.; Liang, S.; Lu, Y.; Huang Chen, S. W.; Guo, W.; Kuo, H. C.; Chen, Z. Mini-LED and micro-LED: promising candidates for the next generation display technology. *Appl. Sci.* **2018**, *8*, 1557.

(5) Lu, S.; Li, J.; Huang, K.; Liu, G.; Zhou, Y.; Cai, D.; Zhang, R.; Kang, J. Designs of InGaN Micro-LED Structure for Improving Quantum Efficiency at Low Current Density. *Nanoscale Res. Lett.* **2021**, *16*, 99.

(6) Wan, R.; Wang, L.; Huang, J.; Yi, X.; Kuo, H. C.; Li, J. Improving the Modulation Bandwidth of GaN-Based Light-Emitting Diodes for High-Speed Visible Light Communication: Countermeasures and Challenges. *Adv. Photonics Res.* **2021**, *2*, No. 2100093.

(7) Hang, S.; Chuang, C. M.; Zhang, Y.; Chu, C.; Tian, K.; Zheng, Q.; Wu, T.; Liu, Z.; Zhang, Z. H.; Li, Q.; Kuo, H. C. A review on the low external quantum efficiency and the remedies for GaN-based micro-LEDs. *J. Phys. D: Appl. Phys.* **2021**, *54*, 153002.

(8) Xu, F. F.; Tao, T.; Liu, B.; Wang, X.; Gong, M. G.; Zhi, T.; Pan, D. F.; Xie, Z. L.; Zhou, Y. G.; Zheng, Y. D. High-Performance semi-polar InGaN/GaN green micro light-emitting diodes. *IEEE Photonics J.* **2019**, *12*, 1−7.

(9) Horng, R. H.; Sinha, S.; Wu, Y. R.; Tarntair, F. G.; Han, J.; Wuu, D. S. Characterization of semi-polar (20-21) InGaN microLEDs. *Sci. Rep.* **2020**, *10*, 15966.

(10) Zhao, G.; Wang, L.; Li, H.; Meng, Y.; Li, F.; Yang, S.; Wang, Z. Structural and optical properties of semi-polar (11-22) InGaN/GaN green light-emitting diode structure. *Appl. Phys. Lett.* **2018**, *112*, No. 052105.

(11) Liu, Y.; Feng, F.; Zhang, K.; Chan, K. W.; Liu, Z.; Kwok, H. S. Low Efficiency Attenuation and Stable Monochromaticity for Non-polar M-Plane Micro-Light-Emitting-Diodes (Micro-LEDs). *Symp. Digest of Tech. Papers* **2022**, *53*, 62−65.

(12) Tu, C. G.; Liao, C. H.; Yao, Y. F.; Chen, H. S.; Lin, C. H.; Su, C. Y.; Shih, P. Y.; Chen, W. H.; Zhu, E.; Kiang, Y. W.; Yang, C. C. Regularly patterned non-polar InGaN/GaN quantum-well nanorod light-emitting diode array. *Opt. Express* **2014**, *22*, A1799−A1809.

(13) Wang, S. W.; Hong, K. B.; Tsai, Y. L.; Teng, C. H.; Tzou, A. J.; Chu, Y. C.; Lee, P. T.; Ku, P. C.; Lin, C. C.; Kuo, H. C. Wavelength tunable InGaN/GaN nano-ring LEDs via nano-sphere lithography. *Sci. Rep.* **2017**, *7*, 42962.

(14) Bai, J.; Wang, Q.; Wang, T. Characterization of InGaN-based nanorod light emitting diodes with different indium compositions. *J. Appl. Phys.* **2012**, *111*, 113103.

(15) Li, K. H.; Fu, W. Y.; Cheung, Y. F.; Wong, K. K.-Y.; Wang, Y.; Lau, K. M.; Choi, H. W. Monolithically integrated InGaN/GaN light-emitting diodes, photodetectors, and waveguides on Si substrate. *Optica* **2018**, *5*, 564−569.

(16) Shi, Z.; Li, X.; Zhu, G.; Wang, Z.; Grünberg, P.; Zhu, H.; Wang, Y. Characteristics of GaN-based LED fabricated on a GaN-on-silicon platform. *Appl. Phys. Express* **2014**, *7*, No. 082102.

(17) Zhang, X.; Li, P.; Zou, X.; Jiang, J.; Yuen, S. H.; Tang, C. W.; Lau, K. M. Active matrix monolithic LED micro-display using GaN-on-Si epilayers. *IEEE Photonics Technol. Lett.* **2019**, *31*, 865−868.

(18) Ley, R. T.; Smith, J. M.; Wong, M. S.; Margalith, T.; Nakamura, S.; DenBaars, S. P.; Gordon, M. Revealing the importance of light extraction efficiency in InGaN/GaN microLEDs via chemical treatment and dielectric passivation. *Appl. Phys. Lett.* **2020**, *116*, 251104.

(19) Hu, X.; Cai, J.; Liu, Y.; Zhao, M.; Chen, E.; Sun, J.; Yan, Q.; Guo, T. Design of inclined omni-directional reflector for sidewall-emission-free micro-scale light-emitting diodes. *Opt. Laser Technol.* **2022**, *154*, No. 108335.

(20) Tian, M.; Yu, H.; Memon, M. H.; Xing, Z.; Huang, C.; Jia, H.; Zhang, H.; Wang, D.; Fang, S.; Sun, H. Enhanced light extraction of the deep-ultraviolet micro-LED via rational design of chip sidewall. *Opt. Lett.* **2021**, *46*, 4809−4812.

(21) Zhou, S.; Zhao, X.; Du, P.; Zhang, Z.; Liu, X.; Liu, S.; Guo, L. J. Application of patterned sapphire substrate for III-nitride light-emitting diodes. *Nanoscale* **2022**, *14*, 4887−4907.

(22) Wuu, D.; Wang, W.; Wen, K.; Huang, S.; Lin, S.; Huang, S.; Lin, C.; Horng, R. H. Defect reduction and efficiency improvement of near-ultraviolet emitters via laterally overgrown GaN on a GaN/patterned sapphire template. *Appl. Phys. Lett.* **2006**, *89*, 161105.

(23) Wang, H.; Wang, L.; Sun, J.; Guo, T. L.; Chen, E. G.; Zhou, X. T.; Zhang, Y. A.; Yan, Q. Role of surface microstructure and shape on light extraction efficiency enhancement of GaN micro-LEDs: A numerical simulation study. *Displays* **2022**, *73*, No. 102172.

(24) Han, D.; Ma, S.; Jia, Z.; Liu, P.; Jia, W.; Dong, H.; Shang, L.; Zhai, G.; Xu, B. Enhanced light extraction efficiency of a InGaN/GaN micro-square array light-emitting diode chip. *Opt. Mater. Express* **2017**, *7*, 3261−3269.

(25) Liu, T.; Li, D.; Hu, H.; Huang, X.; Zhao, Z.; Sha, W.; Jiang, C.; Du, C.; Liu, M.; Pu, X. Piezo-phototronic effect in InGaN/GaN semi-floating micro-disk LED arrays. *Nano Energy* **2020**, *67*, No. 104218.

(26) Zhu, G.; Li, J.; Li, J.; Guo, J.; Dai, J.; Xu, C.; Wang, Y. Single-mode ultraviolet whispering gallery mode lasing from a floating GaN microdisk. *Opt. Lett.* **2018**, *43*, 647−650.

(27) Liu, W. J.; Chen, S. Q.; Hu, X. L.; Liu, Z.; Zhang, J. Y.; Ying, L. Y.; Lv, X. Q.; Akiyama, H.; Cai, Z. P.; Zhang, B. P. Low threshold lasing of GaN-based VCSELs with sub-nanometer roughness polishing. *IEEE Photonics Technol. Lett.* **2013**, *25*, 2014−2017.

(28) Mei, Y.; Weng, G. E.; Zhang, B. P.; Liu, J. P.; Hofmann, W.; Ying, L. Y.; Zhang, J. Y.; Li, Z. C.; Yang, H.; Kuo, H. C. Quantum dot vertical-cavity surface-emitting lasers covering the 'green gap'. *Light: Sci. Appl.* **2017**, *6*, e16199−e16199.

(29) Guo, W.; Meng, H.; Chen, Y.; Sun, T.; Li, Y. Wafer-level monolithic integration of vertical micro-LEDs on glass. *IEEE Photonics Technol. Lett.* **2020**, *32*, 673−676.

(30) Mei, Y.; Xu, R. B.; Xu, H.; Ying, L. Y.; Zheng, Z. W.; Zhang, B. P.; Li, M.; Zhang, J. A comparative study of thermal characteristics of GaN-based VCSELs with three different typical structures. *Semicond. Sci. Technol.* **2017**, *33*, No. 015016.

(31) Lau, K. M.; Wong, K. M.; Zou, X.; Chen, P. Performance improvement of GaN-based light-emitting diodes grown on patterned Si substrate transferred to copper. *Opt. Express* **2011**, *19*, A956−A961.

(32) Wang, J.; Feng, M.; Zhou, R.; Sun, Q.; Liu, J.; Huang, Y.; Zhou, Y.; Gao, H.; Zheng, X.; Ikeda, M.; Yang, H. GaN-based ultraviolet microdisk laser diode grown on Si. *Photon. Res.* **2019**, *7*, B32−B35.

(33) Yang, S.; Xu, H.; Long, H.; Ying, L.; Luo, R.; Zhong, M.; Lu, W.; Hou, X.; Mei, Y.; Zhang, B. GaN-based green resonant-cavity light-emitting diodes with Al mirror and copper plate. *Opt. Lett.* **2022**, *47*, 2858−2861.

(34) Chen, S. W.; Huang, Y. M.; Chang, Y. H.; Lin, Y.; Liou, F. J.; Hsu, Y. C.; Song, J.; Choi, J.; Chow, C. W.; Lin, C. C.; Horng, R. H.; Chen, Z.; Han, J.; Wu, T.; Kuo, H. C. High-bandwidth green semipolar (20−21) InGaN/GaN micro light-emitting diodes for visible light communication. *ACS Photonics* **2020**, *7*, 2228−2235.

(35) Pereira, S.; Correia, M.; Pereira, E.; Trager-Cowan, C.; Sweeney, F.; O'Donnell, K.; Alves, E.; Franco, N.; Sequeira, A. Structural and optical properties of InGaN/GaN layers close to the critical layer thickness. *Appl. Phys. Lett.* **2002**, *81*, 1207−1209.

(36) Cancio, A.; Chang, Y.-C. Quantum Monte Carlo studies of binding energy and radiative lifetime of bound excitons in direct-gap semiconductors. *Phys. Rev. B* **1993**, *47*, 13246.

(37) Chen, W.; Hu, G.; Lin, J.; Jiang, J.; Liu, M.; Yang, Y.; Hu, G.; Lin, Y.; Wu, Z.; Liu, Y.; Zhang, B. High-performance, single-pyramid micro light-emitting diode with leakage current confinement layer. *Appl. Phys. Express* **2015**, *8*, No. 032102.

(38) Zhang, K.; Liu, Y.; Kwok, H.-S.; Liu, Z. Investigation of electrical properties and reliability of GaN-based micro-LEDs. *Nanomaterials* **2020**, *10*, 689.

(39) Mei, Y.; Xie, M.; Xu, H.; Long, H.; Ying, L.; Zhang, B. Electrically injected GaN-based microdisk towards an efficient whispering gallery mode laser. *Opt. Express* **2021**, *29*, 5598−5606.

https://doi.org/10.1021/acsphotonics.2c01366
ACS Photonics 2022, 9, 3967−3973